Published in final edited form as:
J Biomech Eng. 2009 August ; 131(8): 081011. doi:10.1115/1.3148469.

Carpal tunnel expansion by palmarly directed forces to the transverse carpal ligament

Zong-Ming Li, **Jie Tang**, **Matthew Chakan**, and **Rodrigo Kaz**
Hand Research Laboratory Departments of Orthopaedic Surgery and Bioengineering University of Pittsburgh Pittsburgh, PA 15213

Abstract

This study investigated the expansion of the carpal tunnel resulting from the application of palmarly directed forces to the transverse carpal ligament (TCL) from inside the carpal tunnel. Ten fresh-frozen cadaveric hands were dissected to evacuate the carpal tunnel and thus to expose the TCL. A custom lever device was built to apply forces, ranging from 10 to 200 N, to the TCL. Without force application, the carpal tunnel area was 148.4 ± 36.8 mm^2. The force application caused the TCL to form arches with an increase in cross-sectional areas of 33.3 ± 5.6 mm^2 at 10 N and 48.7 ± 11.4 mm^2 at 200 N, representing respective increases of 22.4% and 32.8% relative to the initial carpal tunnel area. The TCL length remained constant under the applied forces. It was found that the TCL arch formation was due to the narrowing of the arch width, which resulted from the migration of the bony insertion sites of the TCL. A geometrical model of the carpal tunnel was then developed to elucidate the relationships among the arch width, TCL length, arch height, and arch area. The model illustrated the effectiveness of carpal tunnel expansion by TCL elongation or arch width narrowing.

Keywords

Transverse carpal ligament; Carpal tunnel; Force; Deformation

INTRODUCTION

The carpal tunnel is a confined space containing the median nerve and nine flexor tendons, and the mechanical properties of the tunnel structure have critical relevance to compression median neuropathy. The transverse carpal ligament (TCL) plays an important role in regulating carpal tunnel mechanics [1]. In particular, hypertrophy of the TCL has been postulated as one of the underlying pathogenic mechanisms of carpal tunnel syndrome [2]. Imaging studies have shown that the TCLs were thickened in individuals with carpal tunnel syndrome [3]. In addition, TCLs associated with carpal tunnel syndrome have been shown to exhibit mucoid change, amyloid deposits, inflammation, fibrocartilagenous metaplasia, and faster growth of contractile cells [4,5], which may alter the mechanical properties of the ligament and create an adverse mechanical environment responsible for compression neuropathy.

Transecting the TCL remains the standard surgical treatment for carpal tunnel syndrome, although preserving the TCL should be considered because this ligament serves important anatomical, biomechanical and physiological functions [1,6,7]. Manipulating carpal tunnel

Correspondence Zong-Ming Li, PhD 210 Lothrop Street, E1641 BST Pittsburgh, PA 15213, U.S.A. Phone: 412 648 1494 Fax: 412 648 8548 zmli@pitt.edu.

mechanics without transecting the TCL, by either myofascial release [8] or using a wearable hand traction device [9], has shown to improve the symptoms of carpal tunnel syndrome. Reconstruction of the TCL after carpal tunnel release has been shown to restore the gliding and pulley mechanisms of the flexor tendons and to improve hand function [6]. Balloon carpal tunnel plasty as a minimally invasive operative procedure has been used to extend the carpal tunnel for the treatment of carpal tunnel syndrome [10]. It is imperative, nevertheless, to understand the mechanics of the carpal tunnel in order for the mechanical properties to be exploited for treatment alternatives.

On the basis of these various results, we hypothesized that the carpal tunnel can be expanded by mechanical manipulation of the TCL. In this study, we investigated the expansion of the carpal tunnel by applying palmarly directed forces to the TCL from inside the carpal tunnel.

METHODS

Ten fresh-frozen cadaveric hands (age 56.2 ± 6.1 years) were used in this study. Medical history indicated no neuromuscular or musculoskeletal disorders to the hand and wrist. The wrist dimensions at the distal wrist crease were 52.6 ± 9.2 mm in width, 34.9 ± 3.9 mm in depth, and 188.3 ± 14.4 mm in circumference. The specimens were transected at 10 cm proximal to the distal wrist crease.

Prior to testing, each specimen was thawed overnight at room temperature prior to testing, and then dissected to expose the TCL. Upon thawing, the specimen was dissected to expose the three distinct portions of the flexor retinaculum: antebrachial fascia (proximal), the TCL (middle) and the distal aponeurosis [1,11]. The TCL was recognized by its transverse fibers and insertions at the pisiform, hook of hamate, tuberosity of scaphoid and ridge of trapezium (Figure 1A). The carpal tunnel was evacuated by removing the flexor tendons and the median nerve (Figure 1B). The exposed TCL was then inscribed by a quadrilateral area with the four vertices denoted by the bony insertion sites. The four vertices were marked on the TCL surface by 0.125 mm thick, 1.6 mm diameter shim stock markers (McMaster Carr, Cleveland, OH) with super glue gel. The center of the marker was slightly indented to enhance the accuracy of digitization.

Upon dissection preparation, the specimen was mounted in a supinated position on a hand support with the wrist extended at approximately 20 degrees (Figure 2). The inner surface of the carpal tunnel excluding the dorsal surface of the TCL was digitized using a MicroScribe digitizer (Immersion Corporation, San Jose, CA). Then, a steel plate (4.2 mm thick and 13.5 mm wide), passing through the carpal tunnel and fixed at both ends, was used to stabilize the specimen. A custom-made lever device was built to apply forces on the TCL. A steel bar was pivoted on a suspended, threaded rod. One end of the bar was to bear a weight and the other end of the bar (ϕ = 10 mm) was inserted to the carpal tunnel. The total length of the lever arm was 450 mm. The lever arm at the TCL side was 150 mm, measuring from the fulcrum to the middle level at the TCL. To fit the stabilization plate and lever bar in the carpal tunnel, the bar end inside the carpal tunnel was thinned by trimming the circular shape to an arc shape. Eight pre-determined force levels (10, 20, 30, 40, 50, 100, 150, and 200 N) were sequentially and individually applied to the TCL. To assess the effect of loading history, the 10 N was applied again after the 200 N force. During each force application, the palmar surface of the TCL was randomly digitized for approximately 1500 data points, covering the inscribed quadrilateral area (Figure 3). In addition, the bony insertion markers and several control points on the stabilization plate were digitized to establish local coordinate systems.

Two local coordinate systems were established for data transformation; one plate coordinate system on the stabilization plate and the bone coordinate system associated with the carpal bones. For the plate coordinate system, which allowed for the measurement of bony migration at the insertion sites, the X-, Y-, and Z-axes pointed in the ulnar, distal, and palmar directions, respectively, and the origin was located on the plate at the level of the distal edge of the TCL. The bone coordinate system, which allowed for definition of TCL arch with respect to the bony insertion sites, was established using the three markers at the insertion sites to the scaphoid, trapezium, and pisiform. The Y-axis was defined by the vector from the scaphoid marker to the trapezium marker, the Z-axis was perpendicular to the plane formed by the three bone markers, the X-axis was formed by the cross-product of Y- and Z-axes; the origin was at the scaphoid marker.

The cross-section of the carpal tunnel was oriented in the plane that was perpendicular to the Y-axis of the bone coordinate system. The cross-section passing through the middle point of the trapezium and scaphoid bone markers was selected for analyses. The total carpal tunnel cross-sectional area was calculated as $A = A_1 + A_2$, where A_1 is formed by the carpal bones assuming a flat TCL and A_2 is formed by the carpal arch above the bony insertion level (Figure 4). To calculate A_1, the digitized data from the inner surface of the carpal tunnel prior to the loading were transformed to the bone coordinate system, which was used to reconstruct the surface of the bony part of the tunnel. The area of this cross-section was calculated by the integration of the bounded region using Matlab (Mathworks, Natick, MA). In addition, the pre-loading A_1 value was assumed to be unchanged for the subsequent loading conditions. To calculate A_2, a set of digitized data during each loading condition was transformed to the plate coordinate system, which was used to reconstruct the TCL surface using a B-Spline surface fitting algorithm. The cross-section of the TCL arch was defined as perpendicular to the Y-axis of the plate coordinate system. In addition, the arch area A_2 was calculated with the exclusion of the cross-sectional area of the TCL tissue because the digitization was performed on the palmar surface of the TCL. The TCL was assumed to have an average thickness of 2 mm [11]. For the TCL arch section, the arch height was defined as the distance between the middle point of the TCL and the line connecting the radial and ulnar edge points (Figure 4). In addition, the arch width was defined as the distance between the radial and ulnar edges of the TCL arch, and the TCL length in the transverse plane was calculated as the path integral of the TCL arch width. Changes in TCL arch height, arch width, TCL length, arch area, and carpal tunnel area were analyzed by one-way repeated measures analyses of variances.

RESULTS

An example of the surface plots of the TCL is shown in Figure 5. The TCL surface was more or less flat when there was no force applied, and the application of a force caused formation of a TCL arch. Figure 6 shows representative cross-sectional curves in the transverse plane, which progressively moved palmarly (in the positive Z direction) with increasing forces. The arch height increased nonlinearly with increasing forces (Figure 7 i), increasing steadily at the lower forces and leveling off at the higher forces. An arch height of 3.2 ± 0.3 mm was attained when the force was 10 N. The maximal force of 200 N led to an arch height of 4.9 ± 0.7 mm. Statistical comparisons showed that the arch height at 30, 40, or 50 N was greater than that at 10 N ($p < 0.05$). The arch height at 100, 150, or 200 N was greater than that at 10, 20, or 30 N ($p < 0.05$), but the heights at 100, 150, and 200 N did not differ from each other. In contrast to the arch height, the arch width decreased with increasing forces (Figure 6, Figure 7 iii). Starting with the arch width (22.0 ± 3.1 mm) without force application, the arch width decreased to 21.3 ± 2.9 mm at 10 N ($p < 0.01$). At the maximal force of 200 N, the arch width was 19.7 ± 2.5 mm. However, the forces did not

significantly change the TCL length ($p = 0.98$; Figure 7 iv), which remained an average length 21.5 mm among the specimens.

Similar to the arch height, the arch area increased with increasing forces (Figure 7 ii). The arch area (A_2) was 33.3 ± 5.6 mm^2 at 10 N, and increased significantly at a force greater than 20 N ($p < 0.05$). The arch area reached to 48.7 ± 11.4 mm^2 at 200 N, but the arch areas at 50, 100, 150, and 200 N were not significantly different from each other. The cross-sectional area defined by the carpal bones (A_1) without an arch (i.e. a flat TCL, $A_2 = 0$) was 148.4 ± 36.8 mm^2. With force application and arch formation, the total cross-sectional area of the carpal tunnel ($A_1 + A_2$) was 181.7 ± 41.2 mm^2 (22.4 % increase) with the 10 N. The tunnel area was 197.1 ± 45.3 mm^2 at 200 N, representing an increase of 32.8% in comparison to the tunnel area without an arch.

A GEOMETRICAL MODEL OF THE CARPAL TUNNEL EXPANSION

Our experimental data showed that the TCL was flat without a force applied to it, which means that the arch width (a_0) is equal to the TCL length (l_0) (Figure 8 i). A carpal arch was formed when a force was applied to the TCL. Theoretically, arch formation can be achieved by elongating the TCL (Figure 8 ii) and/or by moving the TCL edges towards each other (i.e. narrowing the arch. Figure 8 iii).

The TCL arch is assumed to be an isosceles triangle, which is closely approximated given that the force application is concentrated on the middle point of the TCL. If the carpal arch is formed by the TCL elongation (Δl) without the deformation of the carpal bony structure (a constant $a = a_0$), the isosceles length is $(a_0 + \Delta l) / 2$. The height of the isosceles triangle (h) is $\sqrt{\left(\frac{a_0+\Delta l}{2}\right)^2 - \left(\frac{a_0}{2}\right)^2}$, and the arch area ($A_2$) is $\frac{1}{2} \times a_0 \times \sqrt{\left(\frac{a_0+\Delta l}{2}\right)^2 - \left(\frac{a_0}{2}\right)^2}$. Therefore, the arch height and the arch area are functions of TCL elongation (Δl).

A second mechanism of TCL arch formation is the narrowing of arch width. Assuming a constant TCL length (l_0), the base of the isosceles triangle is $a = l_0 - \Delta a$, where Δa is amount of arch width narrowing. The height of the isosceles triangle (h) and the arch area (A_2) are $\sqrt{\left(\frac{l_0}{2}\right)^2 - \left(\frac{l_0 - \Delta a}{2}\right)^2}$ and $\frac{1}{2} \times (l_0 - \Delta a) \times \sqrt{\left(\frac{l_0}{2}\right)^2 - \left(\frac{l_0 - \Delta a}{2}\right)^2}$, respectively. In this case, the arch height and arch area are functions of arch width narrowing (Δa).

According to the experimental results, the initial values of the TCL length and arch width are $l_0 = a_0 = 22.0$ mm. The modeling results show that the arch height and the arch area are sensitive to TCL lengthening or arch width narrowing (Figure 9 i and ii); with a small change in either produce a relatively large increase in arch height (h) and arch area (A_2) (Figure 9 i and ii). For example, a TCL elongation of 0.2 mm ($\Delta l = 0.2$ mm) causes a 1.5 mm arch height and 16.4 mm^2 arch area. Similarly, a decrease of 0.2 mm in the arch width ($\Delta a = 0.2$ mm) causes 1.5 mm arch height and 16.1 mm^2 arch area.

How does the carpal width narrowing affect the cross-sectional area composed by the carpal bones (A_1)? For a geometrical model, the bony cross-section of the carpal tunnel (A_1) is assumed to be a semi-ellipse (Figure 8), whose principal axes are represented by the carpal arch width (a) and twice the carpal depth ($d/2$). The area (A_1) can be calculated as $\frac{1}{2} \times \pi \times \frac{a}{2} \times \frac{d}{2}$, and the perimeter of the half-ellipse (excluding the arch width, a) as

$\frac{1}{2}\times\pi\times\left[3\times\left(\frac{a}{2}+\frac{d}{2}\right)-\sqrt{\left(\frac{3a}{2}+\frac{d}{2}\right)\left(\frac{a}{2}+\frac{3d}{2}\right)}\right]$. With the assumption that the perimeter of the ellipse is constant, d covaries with a. As such, A_1 is a function of the change in a. However, A_1 is insensitive to the change of a; Using the average carpal tunnel depth of 9.5 mm for comparison, the area (A_1) fluctuates only slightly (within 1.3 mm^2) when the tunnel width (a) is decreased by 0-2.5 mm. Therefore, the increase in total area is mainly attributable to the formation of the carpal arch.

COMPARISONS BETWEEN THE EXPERIMENTAL AND MODELING RESULTS

Whereas in theory the carpal tunnel can be expanded by TCL elongation, our experimental data showed that the applied forces did not elongate the TCL ($p = 0.98$). Instead, the arch height and the arch area were obtained by the narrowing of the arch width, conforming to the modeled mechanism illustrated in Figure 8 iii. The arch height and the arch area from the modeled geometry matched well with the experimental data (Figure 10 i and ii). For example, the experimental results showed that when the arch width decreased by 0.73 mm at the force of 10 N, the arch height and the arch area, on average, were 3.2 mm and 33.3 mm^2. The geometrical model (Figure 8 iii) predicts that the arch height and arch area are 2.8 mm and 28.3 mm^2, respectively. In this study, when the arch width decreased by 2.0 mm (at 100 N), the experimental data (arch height 4.6 mm and arch area 46.8 mm^2) almost perfectly matched the modeling results (arch height 4.6 mm and arch area 45.8 mm^2). The root mean square errors for the arch height and arch area were 0.19 mm and 2.1 mm^2, respectively. However, the geometric model that assumed the elliptical shape of the A_1 section overestimated the total area by about 15 mm^2 in comparison to the experimental data (Figure 10 iii).

DISCUSSION

This study investigated the expansion of the carpal tunnel resulting from force application to the TCL. The experimental results showed that force application to the TCL caused the formation of a carpal arch, leading to an increase in carpal tunnel cross-sectional area. Based on the geometrical modeling analyses, the TCL arch can be formed by TCL elongation and/or arch width narrowing. Our experimental results showed that the length of the TCL remained constant under the applied loads. Apparently, the forces applied to the TCL were not high enough to elongate the thick band of the TCL.

Though the carpal tunnel is a stable structure reinforced by its peculiar bony configuration and numerous carpal ligaments, the carpal bones still have considerable mobility. For example, wrist flexion/extension largely results from the motion of the individual carpal bones [12]. Clinical and cadaveric studies have demonstrated that TCL transection may result in abnormal kinematics of the carpal bones [13,14], thought to be possible mechanism contributing to postoperative weakness and pain. In the transverse plane, the motion of the carpal bones can change the carpal arch width. Garcia-Elias et al. showed that the carpal arch width measured between the trapezium and the hook of hamate decreased by 4% and 2% when the wrist flexed and extended, respectively, away from the neutral position [15]. Previous experimental and clinical studies showed that TCL transection caused the carpal arch width to increase by about 10% [15-17]. The widening of the carpal arch after TCL transection suggests that an intact TCL be tensioned to resist carpal arch widening. The existence of such tensioning is consistent with our observation that the TCL was flat when there was no force applied to the TCL. However, when a small load of 10 N was applied to the TCL, the carpal arch width decreased and a considerable palmar arch was formed. It

appears that the carpal bones have some joint play for arch width narrowing and carpal arch formation, flexibility that may be beneficial to the carpal tunnel environment because it helps accommodate the physiological variations in carpal tunnel pressure.

There is a well-established association between carpal tunnel pressure and carpal tunnel syndrome, and a higher carpal tunnel pressure was consistently observed in individuals with carpal tunnel syndrome [18]. Carpal tunnel release effectively reduces carpal tunnel pressure and improves symptoms [19]. After this procedure, the transected edges of the TCL spread apart to allow for increased arch height, leading to an increase in the cross-sectional area of the carpal tunnel [16]. For example, Kato et al. reported that endoscopic carpal tunnel release increased the cross-sectional area by 88 mm^2, most of this change (82 mm^2) was due to the increased palmar arch [17]. These experimental data are consistent with our modeling analyses showing that the arch area (A_2) is sensitive to the variation of the arch width and the bony portion of the carpal tunnel (A_1) is relatively constant. In other words, the increase in carpal tunnel area predominately results from the formation of carpal arch, whether the arch is due to TCL elongation or arch narrowing.

Attempts have been made to manipulate the mechanical properties of the carpal tunnel in order to improve the symptoms of carpal tunnel syndrome. Myofascial release manipulation applied to the carpal tunnels of the individuals with carpal tunnel syndrome was shown to be effective in improving symptoms [8]. A wearable external hand traction device designed to elongate the flexor retinaculum also resulted in improved symptoms [9]. Balloon carpal tunnel plasty was shown to be comparable to open carpal tunnel release in treating carpal tunnel syndrome [10]. However, our results failed to support TCL elongation as an underlying mechanism for these procedures. The clinical results of these intervention and treatment procedures are likely due to mechanisms other than TCL elongation. Our results showed that TCL did not have appreciable elongation with the applied forces, though a previous study reported up to a 2.6 mm elongation when a force was applied to the TCL in the transverse direction for a prolonged period [20]. Still, our experimental data and modeling analyses have demonstrated that the carpal tunnel is expandable via the narrowing of the carpal arch width, even though the TCL maintains a constant length.

The geometrical model captures the relationships among the arch width, TCL length, arch height, and arch area, illustrating that TCL elongation and carpal width narrowing are effective for carpal arch formation and carpal tunnel expansion. For example, either a 1.0 mm increase of the TCL length or a 1.0 mm decrease of the arch width can expand the carpal tunnel by more than 30 mm^2, a >20% increase from the initial total tunnel area. Our experimental results showed that the narrowing of the arch width was responsible for the carpal arch formation, closely matching the predicted results by the model. In estimating the total area of the carpal tunnel, the bony portion of the carpal tunnel (A_1) was assumed to be a semi-ellipse, an assumption that caused a systematic error in over-estimating the area by 15 mm^2 in comparison to the area obtained by digitization (164.1 mm^2 vs. 148.4 mm^2). However, this error does not influence the estimation of the arch area, which is the critical component of carpal tunnel expansion.

There were several limitations in this study. First, the area portion formed by the carpal bones (without the TCL arch) of each specimen was determined prior to loading, and was assumed to be constant when a force was applied to the TCL. It was technically difficult to digitize the carpal tunnel after the specimen was mounted in the testing device with the stabilization plate and the lever bar inside the tunnel. However, analyses based on the geometrical model demonstrated that the area change associated with bony migration and tunnel deformation is relatively small (less than 1.3 mm^2). Therefore, the assumption of constant area was reasonable. Second, the viscoelastic behavior of the carpal tunnel structure

was not considered in this study. However, the viscoelasticity of the TCL is of little concern because it did not show measurable elongation under the applied loads. Furthermore, it does not appear that carpal tunnel deformation was affected by the loading history nor did it undergo permanent deformation. The 10 N force application was repeated at the end of the experiment for each specimen; the arch area (37.3 ± 10.2 mm^2) did not differ from that obtained at the initial 10 N force (33.3 ± 5.6 mm^2, $p > 0.05$).

In summary, we investigated the expansion of the carpal tunnel by applying forces to the TCL in the palmar direction from inside the carpal tunnel. The force application caused the TCL to form a TCL arch so that the carpal tunnel was expanded. The TCL arch was due to the narrowing of the arch width resulting from the migration of the bony insertion sites of the TCL, but not by the elongation of the TCL. A geometrical model, developed to elucidate the relationships among the arch width, TCL length, arch height, and arch area, illustrated that the carpal tunnel can be effectively expanded by either TCL elongation or arch width narrowing.

Acknowledgments

The authors thank Lee Berger, MD, for having stimulating discussions about the expandability of the carpal tunnel and for providing the hand support accessory used in the stretching apparatus. This study was supported by the National Institutes Health (R03AR054510) and the National Fisheries Institute Scholarship Award.

REFERENCES

[1]. Brooks JJ, Schiller JR, Allen SD, Akelman E. Biomechanical and anatomical consequences of carpal tunnel release. Clin Biomech (Bristol, Avon). 2003; 18(8):685–93.

[2]. Moore JS. Biomechanical models for the pathogenesis of specific distal upper extremity disorders. Am J Ind Med. 2002; 41(5):353–69. [PubMed: 12071489]

[3]. John V, Nau HE, Nahser HC, Reinhardt V, Venjakob K. CT of carpal tunnel syndrome. AJNR Am J Neuroradiol. 1983; 4(3):770–2. [PubMed: 6410853]

[4]. Nakamichi K, Tachibana S. Histology of the transverse carpal ligament and flexor tenosynovium in idiopathic carpal tunnel syndrome. J Hand Surg [Am]. 1998; 23(6):1015–24.

[5]. Allampallam K, Chakraborty J, Bose KK, Robinson J. Explant culture, immunofluorescence and electron-microscopic study of flexor retinaculum in carpal tunnel syndrome. J Occup Environ Med. 1996; 38(3):264–71. [PubMed: 8882098]

[6]. Netscher D, Mosharrafa A, Lee M, Polsen C, Choi H, Steadman AK, Thornby J. Transverse carpal ligament: its effect on flexor tendon excursion, morphologic changes of the carpal canal, and on pinch and grip strengths after open carpal tunnel release. Plast Reconstr Surg. 1997; 100(3):636–42. [PubMed: 9283561]

[7]. Mashoof AA, Levy HJ, Soifer TB, Miller-Soifer F, Bryk E, Vigorita V. Neural anatomy of the transverse carpal ligament. Clin Orthop. 2001; (386):218–21. [PubMed: 11347839]

[8]. Sucher BM. Myofascial manipulative release of carpal tunnel syndrome: documentation with magnetic resonance imaging. J Am Osteopath Assoc. 1993; 93(12):1273–8. [PubMed: 8307807]

[9]. Porrata H, Porrata A, Sosner J. New carpal ligament traction device for the treatment of carpal tunnel syndrome unresponsive to conservative therapy. J Hand Ther. 2007; 20(1):20–7. quiz 28. [PubMed: 17254905]

[10]. Berger L, Li ZM. Balloon carpal tunnel plasty: first comparative clinical study. Pittsburgh Orthopaedic Journal. 2006; 17:80.

[11]. Cobb TK, Dalley BK, Posteraro RH, Lewis RC. Anatomy of the flexor retinaculum. J Hand Surg [Am]. 1993; 18(1):91–9.

[12]. Kaufmann RA, Pfaeffle HJ, Blankenhorn BD, Stabile K, Robertson D, Goitz R. Kinematics of the midcarpal and radiocarpal joint in flexion and extension: an in vitro study. J Hand Surg [Am]. 2006; 31(7):1142–8.

[13]. Seradge H, Seradge E. Piso-triquetral pain syndrome after carpal tunnel release. J Hand Surg [Am]. 1989; 14(5):858–62.

[14]. Ishiko T, Puttlitz CM, Lotz JC, Diao E. Scaphoid kinematic behavior after division of the transverse carpal ligament. J Hand Surg [Am]. 2003; 28(2):267–71.

[15]. Garcia-Elias M, Sanchez-Freijo JM, Salo JM, Lluch AL. Dynamic changes of the transverse carpal arch during flexion-extension of the wrist: effects of sectioning the transverse carpal ligament. J Hand Surg [Am]. 1992; 17(6):1017–9.

[16]. Gartsman GM, Kovach JC, Crouch CC, Noble PC, Bennett JB. Carpal arch alteration after carpal tunnel release. J Hand Surg [Am]. 1986; 11(3):372–4.

[17]. Kato T, Kuroshima N, Okutsu I, Ninomiya S. Effects of endoscopic release of the transverse carpal ligament on carpal canal volume. J Hand Surg [Am]. 1994; 19(3):416–9.

[18]. Gelberman RH, Hergenroeder PT, Hargens AR, Lundborg GN, Akeson WH. The carpal tunnel syndrome. A study of carpal canal pressures. J Bone Joint Surg Am. 1981; 63(3):380–3. [PubMed: 7204435]

[19]. Okutsu I, Ninomiya S, Hamanaka I, Kuroshima N, Inanami H. Measurement of pressure in the carpal canal before and after endoscopic management of carpal tunnel syndrome. J Bone Joint Surg Am. 1989; 71(5):679–83. [PubMed: 2732256]

[20]. Sucher BM, Hinrichs RN. Manipulative treatment of carpal tunnel syndrome: biomechanical and osteopathic intervention to increase the length of the transverse carpal ligament. J Am Osteopath Assoc. 1998; 98(12):679–86. [PubMed: 9885488]

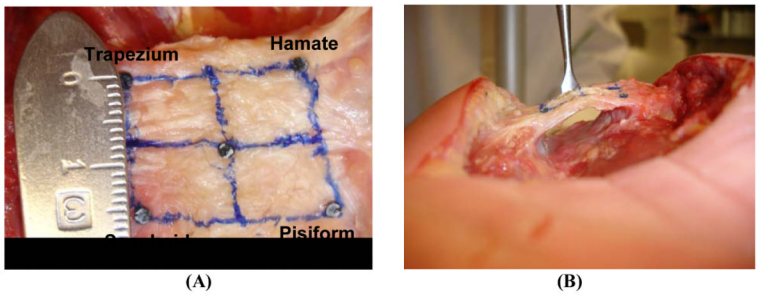

Figure 1.
Cadaveric preparation of the carpal tunnel and TCL viewed palmarly (A) and proximally (B)

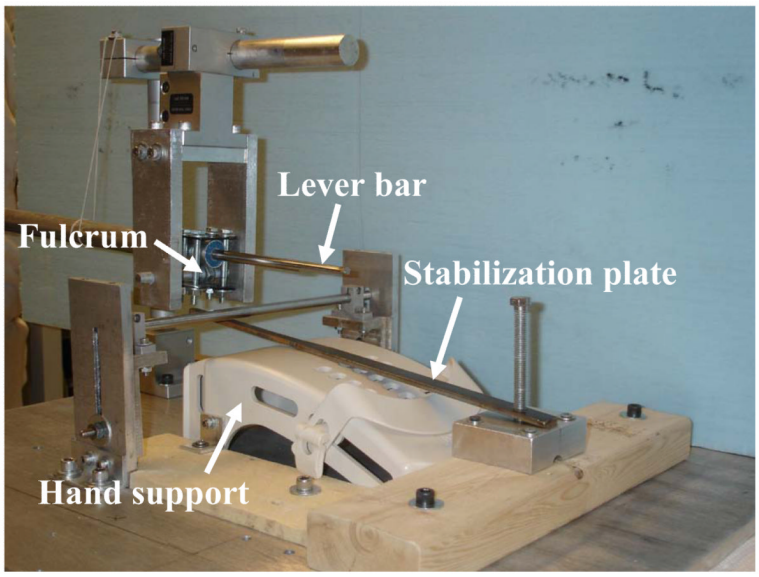

Figure 2.
The custom lever device used to apply forces to the TCL

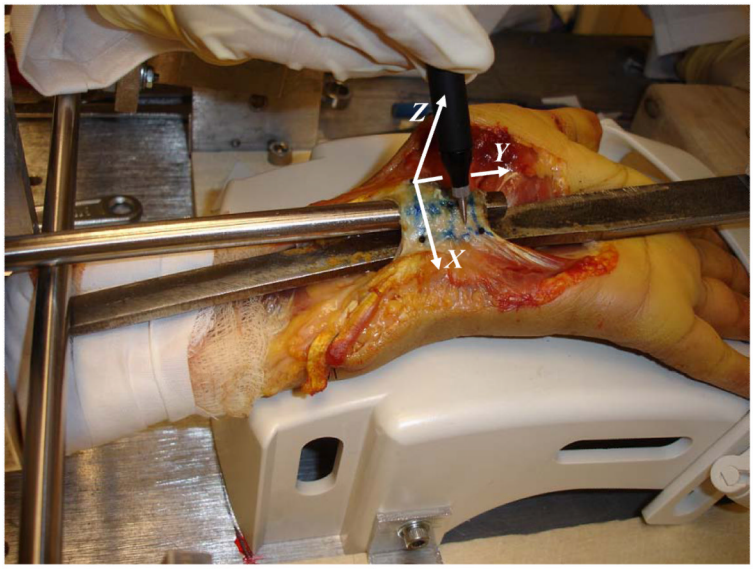

Figure 3.
Digitization of the TCL surface while the TCL was loaded with the lever device

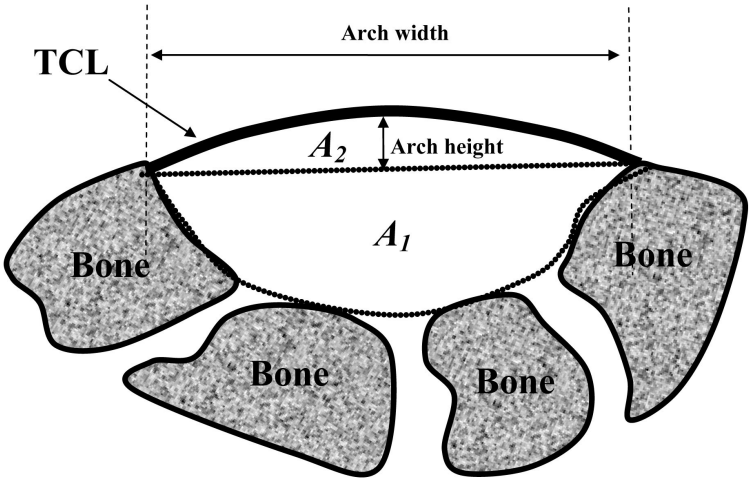

Figure 4.
A schematic of the cross-sectional area of the carpal tunnel is composed of two parts: the baseline area formed by the carpal bones with an assumed flat TCL (A_1) and the area formed by the TCL arch (A_2).

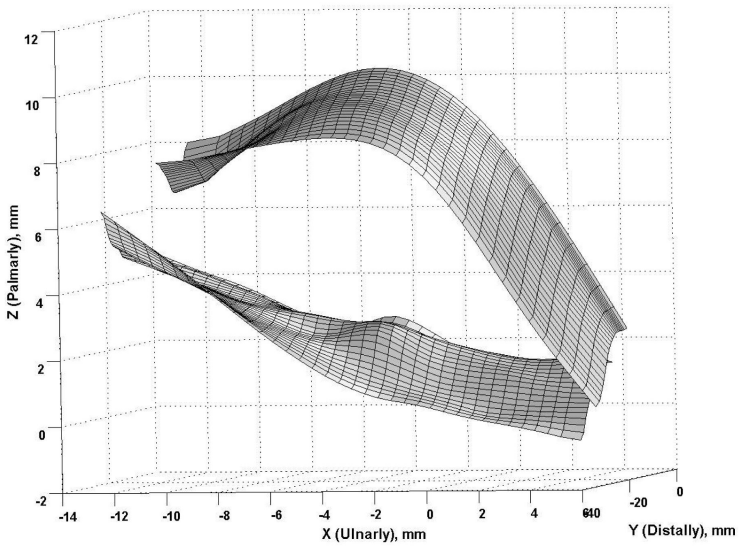

Figure 5.
Representative surface plots of a TCL without force application (the “flat” surface) and the TCL under a 200 N force (the arched surface)

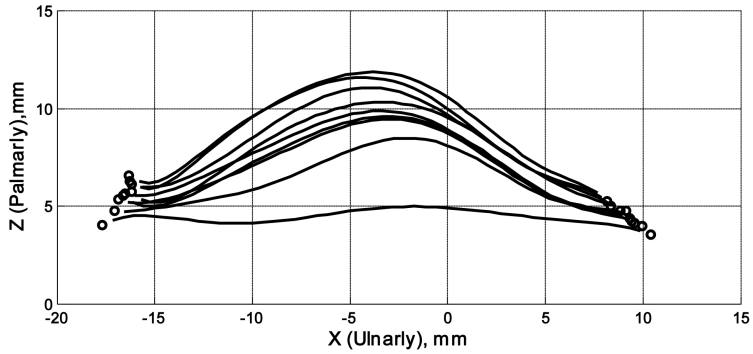

Figure 6.
A representative plot of TCL arch curves in the transverse plane. The curves move progressively upward with increasing forces. The circles denote edge points of the TCL.

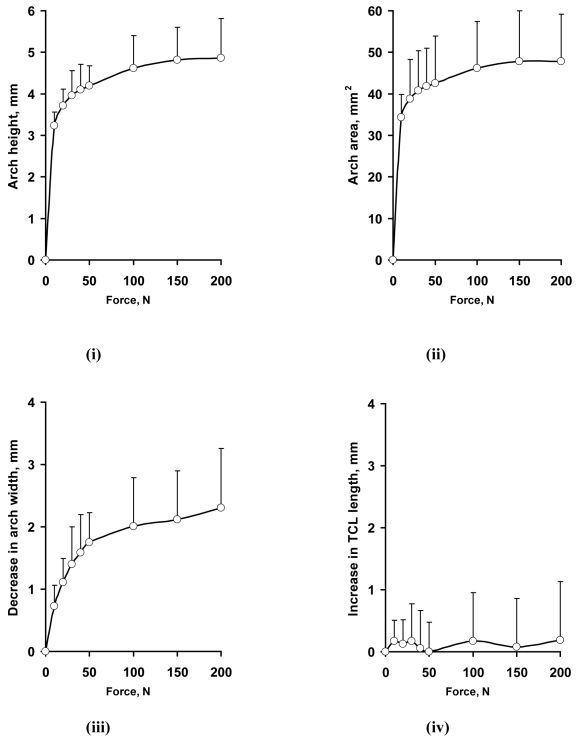

Figure 7.
Changes in arch height (i), arch area (ii), arch width (iii), and TCL length (iv) with increasing forces.

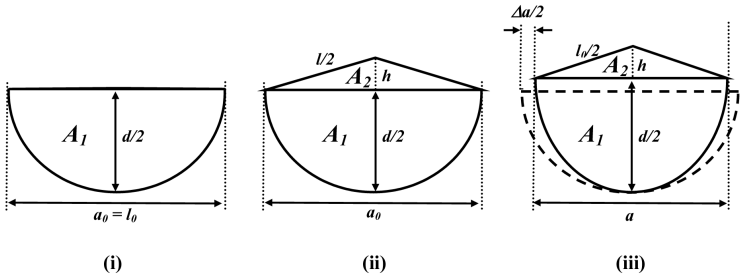

Figure 8.
Geometric representation of the cross-section of the carpal tunnel. (i) Initial carpal tunnel without an arch. (ii) Arch formation by the elongation of the TCL with a constant arch width. (iii) Arch formation by the arch width narrowing assuming a constant TCL length. The enclosed area by the dashed curve and line in (iii) represents the initial carpal tunnel.

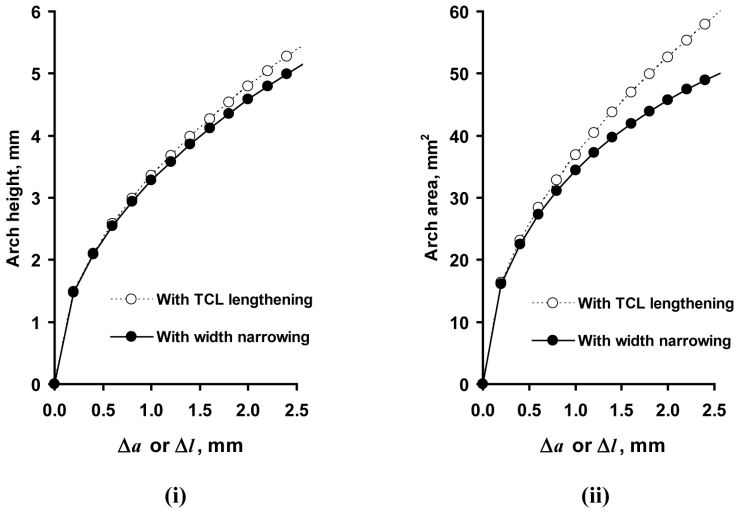

Figure 9.
Arch height (i) and arch area (iii) due to TCL lengthening (Δl) or arch width narrowing (Δa).

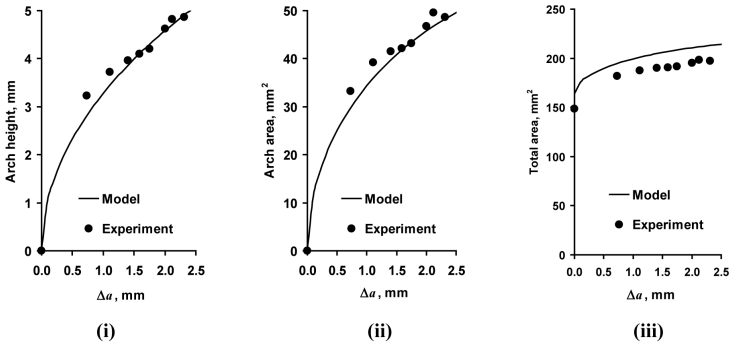

Figure 10.
The changes in arch height (i), arch area (ii), and total area (iii) with the change in arch width (Δa)